THE PENNSYLVANIA STATE UNIVERSITY
SCHREYER HONORS COLLEGE

Axisymmetric CFD Modeling of Contrails Downstream of a Turbofan Engine

SHRESHTH SAXENA
SPRING 2026

A thesis
submitted in partial fulfillment
of the requirements
for a baccalaureate degree in Aerospace Engineering
with honors in Aerospace Engineering

Reviewed and approved* by the following:

Dr. David Hall
Assistant Professor of Aerospace Engineering
Thesis Supervisor

Dr. Sven Schmitz
Boeing/A. D. Welliver Professor of Aerospace Engineering
Thesis Honors Adviser

* Electronic approvals are on file.

ABSTRACT

Aircraft contrails contribute to aviation's climate impact by modifying atmospheric radiation and cloud formation. Predicting the conditions under which contrails form is therefore important for assessing and potentially mitigating these effects. This thesis investigates contrail formation in the wake of a turbofan engine using a combination of engine cycle analysis, computational fluid dynamics (CFD), and the Schmidt-Appleman Criterion. For contrail formation, a thermodynamic cycle analysis of a representative turbofan engine is first performed to determine exhaust properties relevant to contrail formation, including temperature and pressure. A MATLAB code is developed to carry out the engine cycle analysis and to generate exhaust conditions for subsequent modeling. These outputs are then incorporated into a two-dimensional CFD simulation conducted in ANSYS Fluent. The computational grid is generated in Pointwise and imported into Fluent, where the flow field is solved using appropriate turbulence modeling. An approach to predict contrail formation based on the Schmidt-Appleman Criterion is proposed, which may enable identification of contrail regions in the exhaust plume. The proposed approach of coupling engine performance analysis with flow-field simulations provides a foundation for future investigations of contrail mitigation strategies.

TABLE OF CONTENTS

LIST OF FIGURES

LIST OF TABLES

ACKNOWLEDGEMENTS

I would like to express my sincere gratitude to my advisors and mentors, whose guidance and support have been invaluable throughout the course of my academic journey and the completion of this thesis.

First and foremost, I extend my deepest appreciation to Dr. Sven Schmitz for introducing me, during my freshman year, to the critical topics of contrails and sustainability in aviation—subjects that ultimately shaped my academic interests and inspired this work. His continued guidance, encouragement, and insight throughout my time at Penn State have played a pivotal role in both my intellectual and professional development.

I am also profoundly grateful to Dr. Pierce Hart for his mentorship in computational fluid dynamics. His willingness to share his expertise, along with his thoughtful feedback and constructive criticism, significantly strengthened the quality of this thesis. His support not only enhanced my technical skills but also deepened my understanding of the subject matter.

I would like to thank Dr. David Hall for accepting my thesis proposal and for serving as an exceptional mentor throughout this process. His guidance, patience, and encouragement were instrumental in navigating the challenges of this project, and his commitment to my growth made this experience both rewarding and meaningful.

I would also like to extend my sincere appreciation to Dr. Mastaka Okutsu and Dr. Burcu Ozden at Penn State Abington, who provided me with some of my earliest opportunities to engage in research. Their mentorship during the early stages of my academic career played a foundational role in shaping my curiosity and passion for research. Their encouragement and guidance helped me develop confidence in my abilities and set me on a path toward defining my long-term research interests and goals.

I am deeply grateful to my family for their unwavering support, encouragement, and belief in me throughout my academic journey. Their constant motivation, sacrifices, and understanding have been the cornerstone of my achievements. They have supported me through every challenge and celebrated every milestone, providing a foundation of strength that made this accomplishment possible.

I would also like to thank my friends for their encouragement, companionship, and support over the years. Whether through thoughtful conversations, shared challenges, or moments of relief during demanding times, they have made this journey both manageable and meaningful. Their presence has been a source of balance and motivation, and I am truly grateful for their role in helping me reach this point.

Collectively, I have learned a great deal from all of these individuals, both academically and personally. Their mentorship, support, and encouragement have had a lasting impact on my education and growth, and I am sincerely thankful for the knowledge, opportunities, and experiences they have provided.

Nomenclature

B = bypass ratio

CF = Contrail Factor

c_p = specific heat capacity at constat pressure

e = water vapor partial pressure

f = fuel-to-air ratio

G = mixing line slope

M = Mach Number

$\dot{m}$ = mass flow rate

P = static pressure

P_0 = total pressure

Q = Heat

r = pressure ratio

R = universal gas constant

RH = Relative Humidity

T = static temperature

T_0 = total temperature

W = specific power

γ = ratio of specific heat capacities

η = efficiency

Chapter 1

Introduction

Condensation trails (contrails) are cloud-like structures composed of ice crystals formed by aircraft flying in the upper troposphere and lower stratosphere. They are created when water vapor from the environment mixes with water vapor from the exhaust plume and condenses around dust particles, soot, etc. (hereafter referred as condensation nuclei) in the engine exhaust. Environmental water vapor is an important aspect in the formation of contrails, and they are only formed under specific environmental conditions. Humidity and high altitude are two of the main factors responsible for the formation of contrails. Humidity provides water vapor concentration and the high altitude provides the low temperature required for the condensation of the vapor around the condensation nuclei. The ambient temperature range for contrail formation is from -35°C to -60°C [2].

After the Second World War, when contrails were first witnessed [3], studies were carried out to understand and predict contrail formation. One of the earliest studies regarding contrail prediction was done by Appleman in 1953 [3] utilizing a simple mixing-cloud theory. Appleman’s work resulted in a forecasting model that used ambient pressure, temperature, relative humidity and engine efficiency. Pilie and Jiusto [4] further added to this model by establishing a relationship between air parcel vertical motion and contrail formation. Later, Hanson and Hanson [6] further refined this model by predicting contrail formation at lower relative humidities and greater altitudes (lower pressures).

1.1 Schmidt-Appleman Criterion

The Schmidt-Appleman Criterion states that vapor saturation is required for contrail formation, immediate freezing occurs after water droplets are formed and that an ice crystal content of 0.004 g/m^3 is required for a visible contrail [3]. This criterion provides the thermodynamic basis for predicting whether contrail formation is possible given a set of atmospheric and engine conditions. The criterion determines whether the exhaust plume, as it mixes with ambient air, ever reaches saturation with respect to liquid water. Saturation is assessed by comparing the thermodynamic path of the mixing plume against the saturation vapor pressure curve of water, described by the Goff-Gratch equation [10]. Contrail formation is thermodynamically possible when the mixing path intersects this saturation curve as shown in Fig. 1, meaning the plume momentarily becomes supersaturated during the mixing process. The ambient temperature below which this intersection occurs is defined as the critical temperature T_c; if the actual ambient temperature is at or below T_c, contrails can form. Understanding how this intersection is evaluated requires first establishing the saturation curve, then characterizing the mixing path, and finally defining the condition under which the two meet.

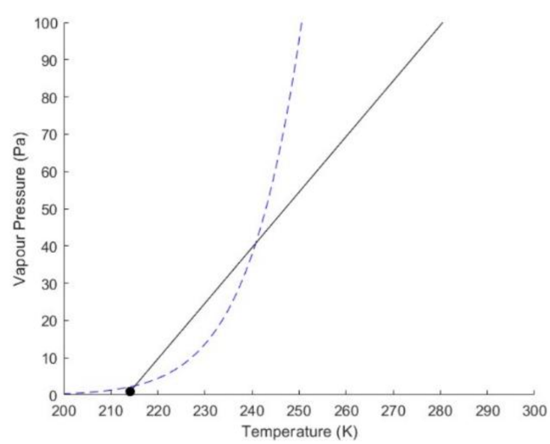

Figure 1 Graph representing the Goff-Gratch vapor pressure formulation (dotted curve) and mixing line (sold line)

The saturation vapor pressure curve defines the maximum partial pressure of water vapor that air can hold at a given temperature before condensation occurs. In this study, the Goff-Gratch formulation [10] is used to represent this curve. The saturation vapor pressure $e_s(T)$ over liquid water is given by

$$\log_{10} e_s = -7.90298\left(\frac{T_s}{T}-1\right) + 5.02808\log_{10}\left(\frac{T_s}{T}\right) - 1.3816\times10^{-7}\left(10^{11.344\left(1-\frac{T}{T_s}\right)}-1\right) \quad (1.1)$$

$$+8.1328\times10^{-3}\left(10^{-3.49149\left(\frac{T_s}{T}-1\right)}-1\right) + \log_{10} e_{s0}$$

where T is the static temperature, $T_s = 373.16$ K is the steam point temperature and e_{s0} is the saturation vapor pressure at T_s. This curve forms the reference against which the thermodynamic state of the mixing plume is compared.

As the hot, moist exhaust gas exits the engine nozzle and mixes isobarically with the cold surrounding atmosphere, it is assumed the thermodynamic state of the mixture traces a straight line in partial pressure-temperature space, connecting the exhaust state at the engine exit to the ambient atmospheric state. This path is referred to as the mixing line [5].

The points along mixing line are described by the dilution factor N [5], which quantifies the degree to which the exhaust has been diluted by ambient air at any point in the wake. N is defined as the ratio of the total plume mass to the mass of fuel burned and increases continuously with downstream distance as more ambient air mixed with the plume. Near the engine exit of a high-bypass turbofan, N typically lies between 50 and 70 [5], and grows rapidly thereafter, reaching values on the order of thousands at the point where liquid saturation is first approached. Each point along the mixing line corresponds to a specific value of N, with the mixture state approaching ambient atmospheric conditions as $N \to \infty$. For conventional jet fuels, the minimum dilution factor required for contrail formation is approximately $N = 15$. Hence, N can be calculated as

$$N = \frac{Q_R(1-\eta)}{c_p(T\text{-}T_{ref})} \tag{1.2}$$

Where Q_R is the heat of combustion of the fuel, η is the overall efficiency of the engine, c_p is the specific heat of air, T is the local temperature in the wake and T_{ref} is the ambient atmospheric temperature at the given altitude.

The linearity of the mixing path arises from the assumption of isobaric, adiabatic mixing with constant specific heat. Schumann [5] formalized this by defining the slope of the mixing line G as the ratio of the change in water vapor partial pressure to the change in temperature during mixing:

$$G = \frac{de_w}{dT} \tag{1.3}$$

where e_w is the partial pressure of water vapor in the plume. This slope can be expressed in terms of engine and atmospheric parameters as

$$G = \frac{EI_{H_2O} c_p P}{\varepsilon Q_R(1-\eta)} \tag{1.4}$$

where P is the ambient pressure and $\varepsilon = 0.622$ is the ratio of molar masses of dry air and water vapor. This formulation shows that G increases with ambient pressure and fuel water content and decreases with increasing efficiency. EI_{H_2O} is the mass of water vapor produced per unit mass of fuel burned.

The contrail factor CF consolidates the fuel and thermal properties of the engine into a single parameter describing the ratio of water vapor added to heat released

$$CF = \frac{EI_{H_2O}\, c_p}{Q_R} \tag{1.5}$$

Appleman [3] originally calculated CF = 0.0336 g(kg·K)$^{-1}$. Peters [11] later refined these values for modern engines, reporting CF = 0.030, 0.034, and 0.039 g(kg·K)$^{-1}$ for non-bypass, low-bypass, and high-bypass turbofan engines respectively. The slope G can equivalently be written in terms of CF as:

$$G = \frac{P * CF}{(1-\eta)\varepsilon} \tag{1.6}$$

The efficiency η quantifies the fraction of combustion heat converted into useful thrust work

$$\eta = \frac{FV}{Q_R \dot{m}_F} \tag{1.7}$$

where F is thrust, V is true airspeed, and $\dot{m}_F$ is the fuel mass flow rate. The remaining fraction $(1-\eta)$ represents the heat deposited into the exhaust plume. It is this fraction that drives plume warming and therefore governs the slope of the mixing line.

Following Hanson and Hanson [6], who incorporated relative humidity into the criterion for improved accuracy at lower pressures, this condition is expressed as:

$$G = \left(\frac{100}{RH}\right)\left(\frac{de_s}{dT}\right)_{T=T_c} \tag{1.8}$$

where RH is the ambient relative humidity in percent.

By fixing the contrail factor based on engine parameters and ambient relative humidity, T_c becomes a function of ambient pressure alone, allowing direct comparison with the local temperature and pressure extracted from the CFD simulation.

1.2 Thesis Objectives

The objective of this research is to increase understanding of engine factors responsible for contrail formation using computational fluid dynamics (CFD) to predict and model contrail formation in the wake of a high bypass turbofan engine. To that end, an engine cycle analysis is carried out, the results of which are applied in CFD coupled with the Schmidt-Appleman criterion for contrail formation. This research makes use of a Reynolds-Averaged Navier-Stokes (RANS) solver to carry out simulations. Contrails are major contributors to the aviation industry's environmental impact [1] and hence understanding the process behind their formation and factors responsible is an important step to create mitigation strategies. Contrails are responsible for around 2/3 of the aviation industry's contribution to ERF, much more than CO_2 emissions [1].

1.3 Thesis Outline

Section 2 discusses the methodology for this research, including a description of engine cycle analysis for a typical high bypass turbofan engine and CFD modeling and provides recommendations for the Schmidt-Appleman Criterion application. Chapter 3 discusses results of the analysis. Chapter 4 concludes the paper and provides recommendations for future work.

Chapter 2

Methodology

This chapter describes the engine cycle analysis and CFD modeling approach developed to support contrail formation prediction. Engine cycle analysis, described in Section 2.1, was carried out to obtain engine exhaust conditions. These exhaust conditions informed boundary conditions for a 2D axisymmetric CFD simulation mesh created in pointwise and exported to ANSYS Fluent as will be discussed in Section 2.2.

2.1 Engine Cycle Analysis

A turbofan engine thermodynamic cycle analysis [8] was performed to determine engine performance and exhaust properties [8] relevant to contrail formation. This analysis models each major engine component using one-dimensional, steady-flow assumptions and standard gas turbine performance relations. Outputs from this analysis are later used as boundary conditions and inputs for the computational fluid dynamics simulations and Schmidt–Appleman Criterion evaluation.

The turbofan engine is modeled as a sequence of thermodynamic states corresponding to stations between engine components, including inlet, fan and bypass duct, compressor, combustor, turbine, and exhaust nozzles as shown in Fig. 3. The station numbering and flow progression used in this analysis are as follows:

- Freestream static conditions to inlet stagnation conditions ($a \rightarrow 0a$)
- Inlet diffusion ($0a \rightarrow 02$)

- Fan and bypass compression ($02 \rightarrow 08$)
- Core compression ($02 \rightarrow 03$)
- Combustion ($03 \rightarrow 04$)
- Turbine expansion ($04 \rightarrow 05$)
- Core nozzle expansion ($05 \rightarrow 06$)
- Bypass nozzle expansion ($08 \rightarrow 8$)

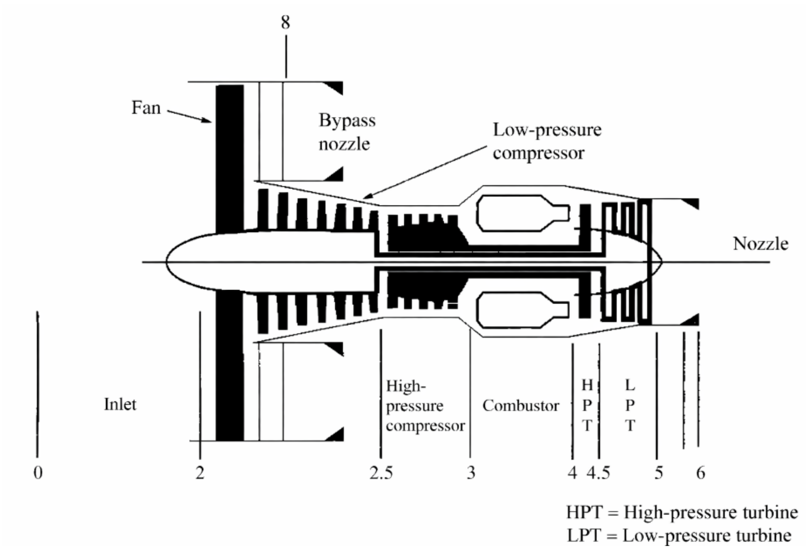

Figure 2 Turbofan engine schematic with numbered and labeled stages [9]

The engine cycle is defined using prescribed design parameters, including component pressure ratios, efficiencies, ratio of specific heats as shown in Table 1 [7] and maximum turbine inlet temperature. The working fluid is modeled as a calorically perfect gas with constant specific heats for each engine section. Separate ratios of specific heats and specific heat capacities are used for the fan, compressor, and combustor to account for temperature-dependent variations in specific heat of the working fluid.

Table 1 NASA N+3 Engine component parameters [7]

Component	Stagnation Pressure ratio (r), Efficiency (η)	Ratio of Specific heats (γ)
Inlet	r_d= 0.998	γ_d= 1.40094
Fan	η_f= 0.9689	γ_f= 1.40094
Fan Nozzle	r_{fn}= 0.9975	γ_{fn}= 1.40067
Compressor	η_c= 0.87	γ_c= 1.396
Combustor	r_c= 0.96, η_b= 0.999	γ_b= 1.34875
Turbine	η_t= 0.91	γ_t= 1.302
Core Nozzle	r_n= 0.9999	γ_n= 1.34569

Freestream static pressure P_∞ and temperature T_∞ are converted to stagnation conditions based on the flight Mach number M:

$$P_{0a} = P_a\left(1 + M^2\frac{\gamma_d - 1}{2}\right)^{\frac{\gamma_d}{\gamma_d-1}} \tag{2.1}$$

$$T_{0a} = T_a\left(1 + M^2\frac{\gamma_d - 1}{2}\right). \tag{2.2}$$

Inlet pressure losses are accounted for using a diffuser pressure recovery factor r_d:

$$P_{02} = r_d P_{0a} \tag{2.3}$$

whereas temperature remains the same as

$$T_{02} = T_{0a}\,. \tag{2.4}$$

The fan increases the stagnation pressure and temperature of the bypass flow. The fan exit pressure is calculated using fan pressure ratio and the fan exit stagnation temperature is calculated using the fan pressure ratio and ratio of specific heats:

$$P_{08} = p_{rf} r_{fn} P_{02} \tag{2.5}$$

$$T_{08} = \left(\frac{p_{rf}^{\frac{\gamma_{fn}-1}{\gamma_{fn}}} - 1}{\eta_f} + 1 \right) T_{02}. \tag{2.6}$$

The fan specific heat is given by

$$c_{pf} = \frac{\gamma_f R}{\gamma_f - 1} , \tag{2.7}$$

where *R* is the universal gas constant. The fan specific power is then calculated as:

$$W_{sf} = B c_{pf} (T_{o8} - T_{o2}) \tag{2.8}$$

where *B* is the bypass ratio.

The core compressor raises the stagnation pressure and temperature of the core flow according to the compressor pressure ratio and the ratio of specific heats as:

$$P_{03} = p_{rc} P_{02} , \tag{2.9}$$

$$T_{03} = \left(\frac{p_{rc}^{\frac{\gamma_c-1}{\gamma_c}} - 1}{\eta_c} + 1 \right) T_{02} . \tag{2.10}$$

The compressor specific heat capacity is defined as:

$$c_{pc} = \frac{\gamma_c R}{\gamma_c - 1} . \tag{2.11}$$

The specific compressor power is:

$$\dot{W}_{sc} = c_{pc}(T_{o3} - T_{o2})\,. \tag{2.12}$$

The combustor is modeled by specifying a maximum turbine inlet temperature T_{o4} and a pressure loss represented by the combustor pressure ratio r_c:

$$P_{o4} = r_c P_{o3} \tag{2.13}$$

$$T_{o4} = T_{max} \tag{2.14}$$

The fuel-to-air ratio is calculated from an energy balance across the combustor

$$f = \frac{T_{o4} - T_{o3}}{\eta_b \frac{Q_R}{c_{pb}} - T_{o4}}\,, \tag{2.15}$$

where Q_R is the fuel heating value and the combustor specific heat capacity is

$$c_{pb} = \frac{\gamma_b R}{\gamma_b - 1}\,. \tag{2.16}$$

The turbine extracts sufficient work to drive both the compressor and the fan. A power balance is enforced between the turbine and the rotating components upstream. The turbine specific work requirement is given by

$$\dot{W}_{st} = \dot{W}_{sc} + \dot{W}_{sf}\,, \tag{2.17}$$

where $\dot{W}_{st}$ is the specific power required by the turbine.

The turbine stagnation temperature is determined from an energy balance that accounts for the presence of fuel in the core flow

$$T_{05} = T_{04} - \frac{W_{st}}{(1+f)c_{pt}}, \tag{2.18}$$

where the turbine specific heat capacity is

$$c_{pt} = \frac{\gamma_t R}{\gamma_t - 1} \; . \tag{2.19}$$

The turbine exit stagnation pressure is calculated using the turbine efficiency η_t and assuming a non-ideal expansion process

$$P_{05} = P_{04}\left[1 - \left(\frac{1 - {T_{05}}/{T_{04}}}{\eta_t}\right)\right]^{\frac{\gamma_t}{\gamma_t - 1}} \tag{2.20}$$

Downstream of the turbine, the core flow passes through the core nozzle, where it is expanded to produce thrust. A nozzle pressure ratio is used to account for losses within the nozzle;

$$P_{06} = r_n P_{05} \; . \tag{2.21}$$

The stagnation temperature is assumed to remain constant across the nozzle:

$$T_{06} = T_{05} \; . \tag{2.22}$$

The exit Mach number of the core flow is calculated using isentropic relations, assuming expansion to ambient pressure P_a:

$$M_8 = \sqrt{\frac{2}{\gamma_d - 1}\left[\left(\frac{P_{08}}{P_a}\right)^{\frac{\gamma_{fn}-1}{\gamma_{fn}}} - 1\right]}\,. \tag{2.23}$$

The core nozzle exit static temperature is

$$T_8 = \frac{T_{o8}}{1 + \frac{(\gamma_f - 1)}{2} {M_8}^2}\,. \tag{2.24}$$

The core exhaust velocity is calculated from the exit Mach number and static temperature:

$$u_{ef} = M_8\sqrt{\gamma_f R T_8} \tag{2.25}$$

The bypass flow exits the engine through the bypass nozzle, where it is expanded to ambient pressure and generates a significant portion of the overall thrust. The bypass nozzle exit Mach number is computed using the stagnation-to-ambient pressure ratio:

$$M_6 = \sqrt{\frac{2}{\gamma_n - 1}\left[\left(\frac{P_{06}}{P_a}\right)^{\frac{\gamma_n-1}{\gamma_n}} - 1\right]}\,. \tag{2.26}$$

The bypass nozzle exit static temperature is then calculated as

$$T_6 = \frac{T_{o6}}{1 + \frac{(\gamma_f - 1)}{2} {M_6}^2}\,. \tag{2.27}$$

The bypass exhaust velocity is

$$u_e = M_6\sqrt{\gamma_f R T_6}\,. \tag{2.28}$$

Because the bypass flow has a lower temperature and higher mass flow rate than the core flow, it influences plume mixing and dilution, which are critical factors in contrail formation.

To calculate relevant performance metrics for our case, we must obtain the thermal and propulsive efficiency, which are

$$\eta_{th} = \frac{(1+f)({u_e}^2 - u^2) + B\left({u_{ef}}^2 - u^2\right)}{2Q_R f}\,, \tag{2.29}$$

$$\eta_p = \frac{2u\left(\frac{T}{\dot{m}_a}\right)}{(1+f)({u_e}^2 - u^2) + B\left({u_{ef}}^2 - u^2\right)}\,. \tag{2.30}$$

where η_{th} and η_p are thermal efficiency and propulsive efficiency respectively T is the thrust and $\dot{m}_a$ is the total mass flow rate and $T/\dot{m}_a$ calculated as

$$T/\dot{m}_a = (1+f)u_e + Bu_{ef} - (1+B)u \tag{2.31}$$

Multiplying the thermal and propulsive efficiencies gives us overall efficiency

$$\eta = \eta_{th}\eta_p \tag{2.32}$$

The combustion process adds chemical energy to the working fluid at a rate determined by the lower heating value (LHV) of the fuel. For JP-4 fuel, Q_R is 43 MJ/kg [5].

The total chemical energy added to the combustor per unit mass of fuel is therefore

$$q_{in} = \eta_b Q_R \tag{2.33}$$

where η_b is the combustion efficiency.

However, not all of this energy remains as thermal energy in the exhaust wake. A portion of the chemical energy is converted into useful propulsive work and kinetic energy of the jet. The fraction converted into useful thrust power is represented by the overall engine efficiency η, obtained from the cycle analysis.

The thermal energy remaining in the exhaust wake per unit mass of fuel is therefore

$$Q = \eta_b Q_R (1-\eta) \tag{2.34}$$

This represents the portion of chemical energy that ultimately manifests as elevated exhaust temperature, turbulent mixing heating and entropy generation in the plume.

Contrail formation is driven by the addition of water vapor to the ambient atmosphere. The mass of water produced per unit mass of fuel is determined from the stoichiometric combustion chemistry.

JP-4 fuel may be approximated as a hydrocarbon with empirical formula $CH_{1.93}$. The balanced stoichiometric combustion reaction in dry air is:

$$CH_{1.93} + 1.4825O_2 + 3.76N_2 \rightarrow CO_2 + 0.965H_2O + 5.57N_2$$

From hydrogen conservation, the number of moles of water produced per mole of fuel is:

$$n_{H_2O} = \frac{1.93}{2} = 0.965 \tag{2.35}$$

The molecular weight of the fuel is:

$$M_f = 12 + 1.93(1) = 13.93 \text{ kg/kmol}$$

The mass of water produced per kilomole of fuel is:

$$m_{H_2O} = 0.965 \times 18 = 17.37 \text{ kg/kmol fuel}$$

Therefore, the water produced per unit mass of fuel is:

$$\frac{m_{H_2O}}{M_f} = 1.247 \text{ kg H}_2\text{O per kg fuel}$$

This value corresponds to the emission index of water vapor which is consistent with published values (1.25 kg H_2O per kg fuel) for conventional aviation fuels ($CH_{1.94}$) [5].

The core and bypass nozzle exit conditions define the initial thermodynamic and velocity fields entering the wake region downstream of the engine. The exhaust temperatures, and pressures obtained from the cycle analysis are used as inputs to the computational fluid dynamics simulations.

2.2 CFD Analysis

To model the exhaust plume development and mixing processes relevant to contrail formation, a two-dimensional axisymmetric computational domain was used. This approach provides a balance between physical fidelity and computational efficiency while capturing the dominant flow physics in the near and intermediate-field regions downstream of the engine exhaust.

The domain consists of distinct inlet regions representing the engine core exhaust, bypass exhaust, and freestream flow, followed by a sufficiently long downstream region to allow for plume mixing with the ambient atmosphere. Axisymmetry is assumed about the engine centerline, which is appropriate for a straight, isolated engine exhaust operating under cruise conditions. Two nozzles are modeled as walls between the core and bypass, and bypass and freestream flow respectively to allow each of the separate flow fields to mix properly and form physical shear layers. The flow is assumed to be steady, compressible, and turbulent. Chemical reactions and ice microphysics are not modeled explicitly; instead, contrail formation prediction is proposed using a thermodynamic criterion based on local flow properties. A schematic of the computational domain and boundary condition layout is shown in Fig. 4.

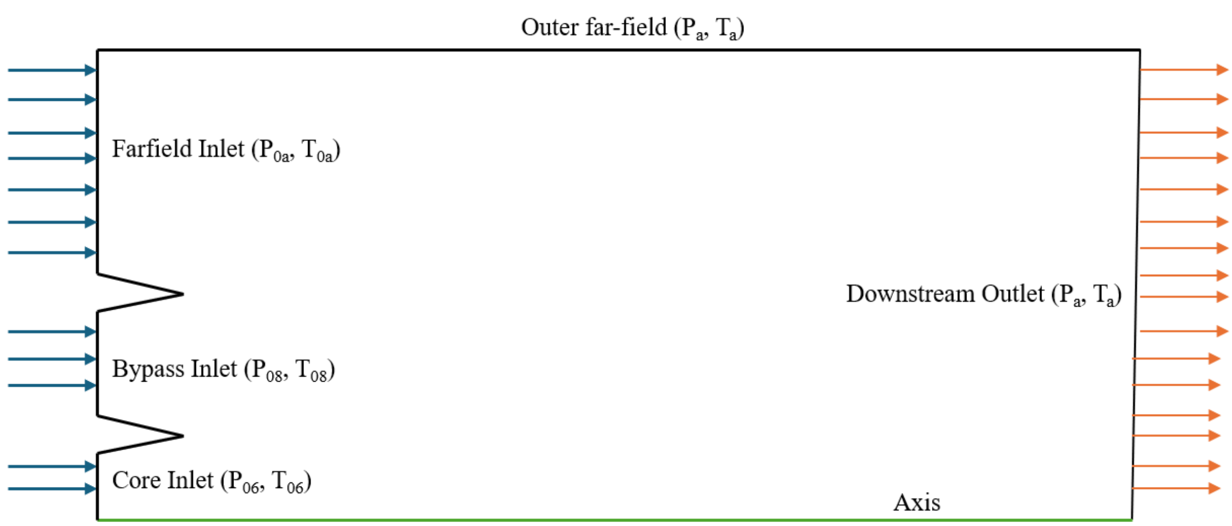

Figure 3 2D axisymmetric domain schematic and boundary conditions

A structured, multi-block mesh was generated using Pointwise to ensure control over grid resolution in key regions such as near the walls and inlets. Separate mesh blocks were created for the core exhaust, bypass exhaust, and surrounding freestream, allowing localized refinement near shear layers where strong velocity and temperature gradients are expected as shown in Fig. 5.

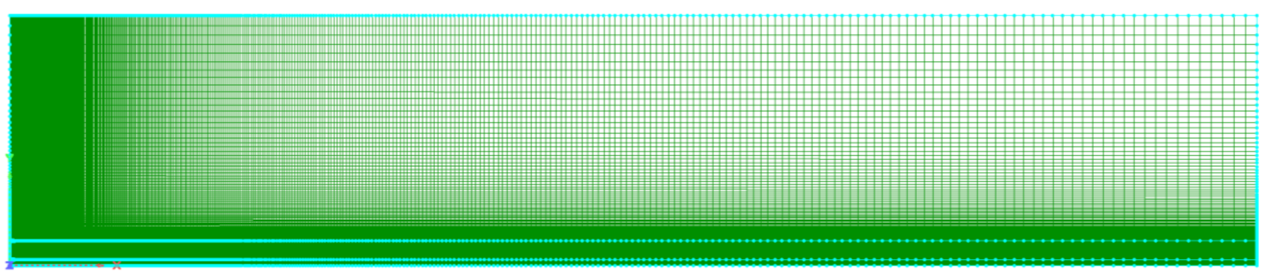

Figure 4 Mesh as displayed in Pointwise

Grid spacing was refined in the near-exhaust region to capture mixing, while coarsened downstream to reduce computational cost. Mesh quality was assessed within Pointwise using standard metrics including cell skewness, aspect ratio, and orthogonality. All cells satisfied recommended quality thresholds for compressible turbulent flow simulations, with a maximum aspect ratio of 68.09 and a maximum skewness of 0.08.

The simulations were performed in ANSYS Fluent using a density-based, steady-state solver suitable for compressible flow. Air was modeled as an ideal gas. Viscosity was modeled using a Reynolds-averaged Navier–Stokes (RANS) SST k-omega approach.

Boundary conditions were specified as follows:

- **Core exhaust inlet:** Pressure inlet with specified total pressure and total temperature obtained from the engine cycle analysis corresponding to core nozzle exit.
- **Bypass exhaust inlet:** Pressure inlet with total conditions corresponding to the bypass nozzle exit.
- **Freestream inlet:** Pressure inlet representing ambient cruise conditions.
- **Outlet boundary:** Static pressure outlet located far downstream.
- **Upper boundary:** Pressure far-field to allow entrainment of ambient flow.
- **Centerline:** Axis boundary condition.

Solver relaxation factors and Courant number were adjusted as needed to ensure numerical stability. The solver was set to a first order accuracy and convergence was assessed based on residual reduction and stabilization of key integral flow equations such as continuity and energy equation.

Chapter 3

Results and Discussion

The turbofan engine cycle analysis was performed using the thermodynamic model described in Chapter 2. For the purposes of this study, the NASA N+3 engine [7] was used as a case to implement into CFD and engine cycle analysis. The properties of the engine were used as inputs for the engine cycle analysis and the resulting values for total pressure and total temperature were compared to those given in the engine manual and errors for the values ranged from 0.003% to 17.8% for pressure and 0% to 12.6% for temperature as can be seen in Table 2.

Table 2 NASA N+3 engine properties at 35000ft and M=0.8 compared between given and obtained data

Station	**Stagnation Pressure, P_0 (Pa)**		**Stagnation Temperature, T_0 (K)**	
	NASA [7]	**Current Model**	**NASA [7]**	**Current Model**
Inlet Entrance	36349	36352	246.9	246.9
Fan Entrance	36280	36279	246.9	246.9
Compressor Exit	1.8246E6	1.8670E6	827.5	830.9
Burner Exit	1.7501E6	1.7923E6	1634.1	1634.1
Turbine Exit	38535	45045	692.6	779.8
Core Nozzle exit	**38162**	**45040**	**692.6**	**779.8**
Fan Nozzle exit	**45623**	**47045**	**265.3**	**266.7**

The engine cycle analysis produced key performance metrics including specific thrust, thrust specific fuel consumption (TSFC), thermal efficiency, propulsive efficiency, and overall efficiency listed in Table 3 with an error of nearly 17-18%. The CFD model provided important parameters such as pressure and temperature downstream of the core and bypass nozzles. These parameters are critical for contrail analysis because they determine the thermodynamic state of the exhaust plume prior to mixing and also during mixing with the ambient atmosphere.

Table 3 Engine performance metrics

	Current Method	**NASA [7]**
Specific thrust	78.87 N/kg	67.37 N/kg
TSFC	0.37954 lb/hr/lbf	0.4644 lb/hr/lbf
Thermal efficiency	0.62	0.402
Propulsive efficiency	0.828	0.868
Overall efficiency	0.513	0.349

The heat released during combustion was determined using the fuel lower heating value of 43 MJ/kg [5]. Since only a portion of this energy is converted into propulsive work, the remainder contributes to heating of the exhaust plume. The effective heat added to the wake per unit mass of fuel is therefore given by

$$Q_{\mathrm{wake}} = 24.639\ \mathrm{MJ/kg}$$

These two parameters– heat released to the wake and water vapor production determine the slope of the plume mixing line described by Appleman [3] and the resulting thermodynamic conditions within the exhaust plume.

Contrail formation was evaluated using the Schmidt–Appleman criterion (SAC) [3], which determines whether mixing between aircraft exhaust gases and ambient atmospheric air leads to saturation with respect to liquid water.

The CFD simulation was conducted in ANSYS Fluent using a two-dimensional axisymmetric representation of the engine exhaust plume interacting with the surrounding freestream atmosphere. The simulations produced detailed flow field data including pressure and temperature distributions downstream of the engine exhaust. The total pressure contours indicate expansion of the exhaust jet immediately downstream of the nozzle exit, followed by pressure drop as the plume mixes with the surrounding freestream air.

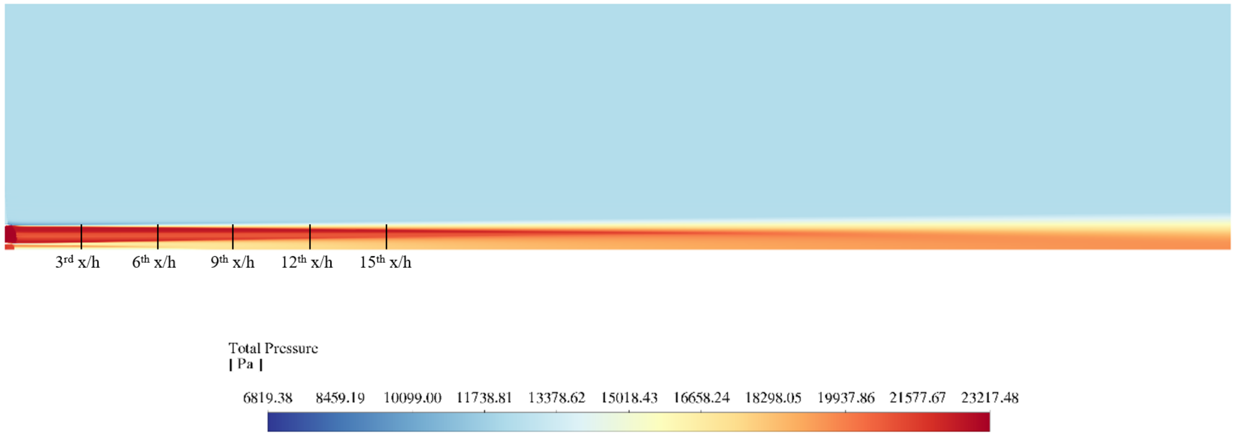

Figure 5 Total Pressure contour depicting mixing in the wake at 35,000ft

The total temperature contours shown in Fig. 7 illustrate the high-temperature exhaust core emerging from the engine nozzle. As the plume propagates downstream, entrainment of ambient air leads to cooling of the exhaust gases. The resulting temperature gradients define the thermodynamic mixing region where contrail formation may potentially occur.

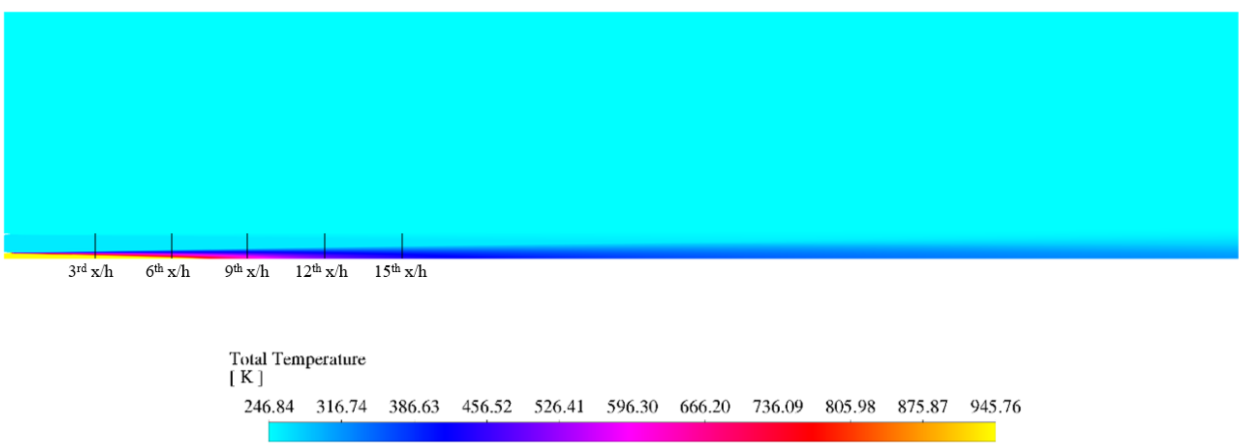

Figure 6 Total temperature contour depicting mixing in the wake at 35,000ft

Explicit contrail formation criteria were not evaluated within the current simulation framework; the temperature field provides a clear indication of the spatial region where plume temperatures approach atmospheric conditions and mixing becomes significant.

Because the current CFD model does not simulate water vapor condensation or ice nucleation processes, contrail formation zones may instead be inferred through analysis of thermodynamic conditions. The CFD results indicate that contrail formation conditions primarily occur in the near-wake region downstream (around x/h= 15 to 18) of the nozzle exit, where turbulent mixing between the exhaust plume and the freestream atmosphere is strongest.

Static pressure and static temperature are extracted along vertical lines (shown in Fig. 5 and 6) at multiple streamwise locations downstream of the nozzle exit as shown in Fig. 7 and 8. The pressure field remains close to ambient conditions beyond a short downstream distance, which is consistent with the assumption of isobaric (static pressure) plume mixing used in the Schmidt–Appleman analysis. These lines span the radial extent of the domain from the axis of symmetry to the outer far-field boundary, capturing the full range of flow conditions from the hot exhaust core through the bypass stream and into the ambient freestream. Each sampling location therefore yields a profile of (P, T) pairs that represent the local thermodynamic state of the plume at that downstream distance. This approach allows the evolution of plume conditions to be tracked spatially as the exhaust mixes and cools with increasing downstream distance.

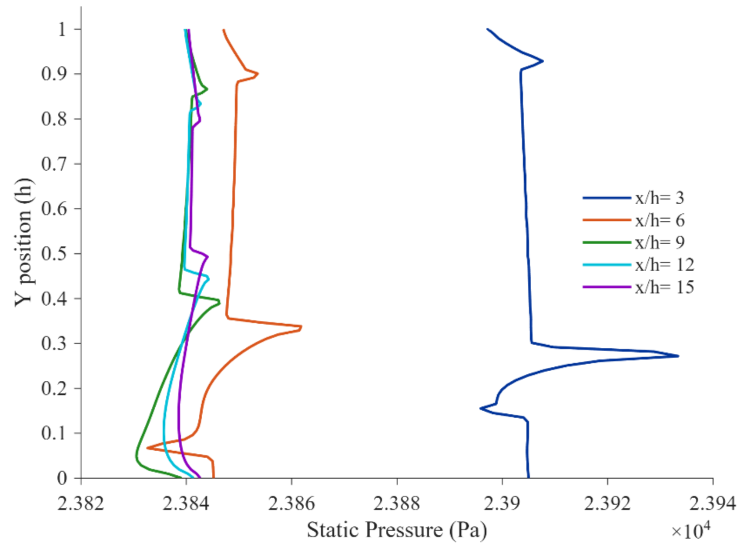

Figure 7 Static Pressure at streamwise locations in the wake

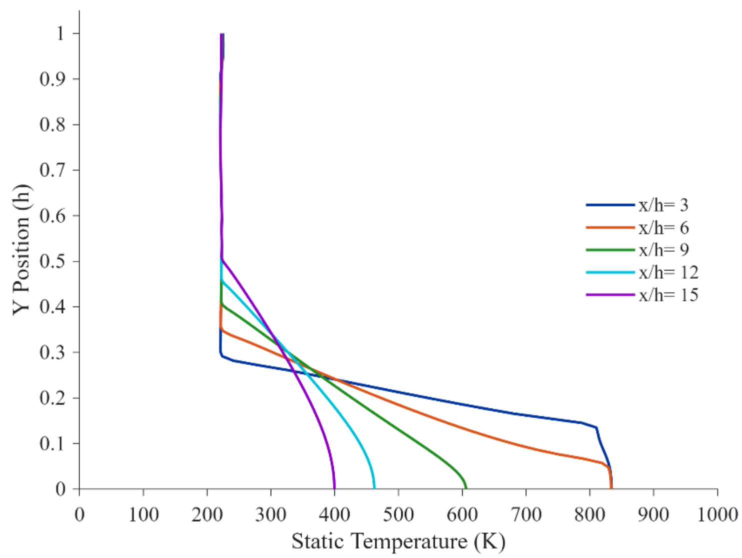

Figure 8 Static Temperature at streamwise locations in the wake

At each extracted (*P, T*) point, the local water vapor partial pressure e_p may be computed using the framework established by Schumann [5]. The water mass fraction of the mixed plume can be calculated using the fuel emission index and fuel to air ratio as

$$m_p = \frac{f\ EI_{H_2O}}{1+f}$$

where f is the fuel-to-air ratio calculated from the engine cycle analysis and EI_{H_2O} is the emission index of water vapor for JP-4 fuel. The corresponding water vapor partial pressure is obtained from

$$e_p = \frac{P\, m_p}{N\varepsilon}$$

where $\varepsilon = 0.622$ is the ratio of molar masses of dry air and water vapor [5]. This yields a coordinate pair for each CFD data point, representing the thermodynamic state of the plume at that location in the wake as seen in Fig. 9.

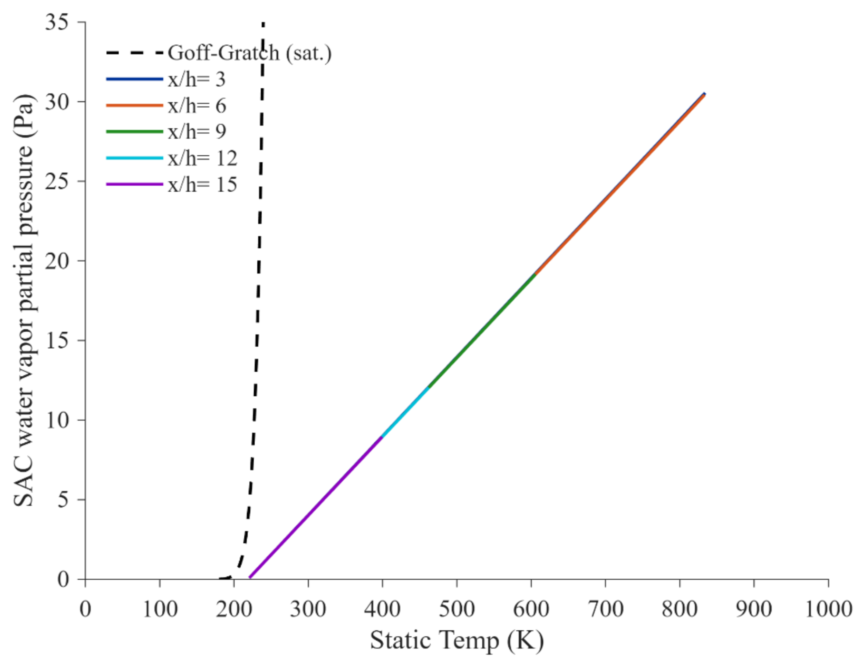

Figure 9 Mixing Line graph

Chapter 4

Conclusion

This thesis proposed an approach for contrail formation prediction for a high-bypass turbofan engine through a combined thermodynamic and computational fluid dynamics approach.

A turbofan engine cycle analysis was first performed to determine key exhaust parameters such as temperature, pressure, exhaust velocity, water vapor production, and heat release. The analysis showed that combustion of JP-4 fuel produces approximately 1.44 kg of water vapor per kilogram of fuel burned, while a significant portion of the fuel's chemical energy remains in the exhaust plume as thermal energy. These factors strongly influence the slope of the plume mixing line and therefore the critical temperature required for contrail formation.

A two-dimensional axisymmetric CFD simulation of the engine exhaust plume was then performed in ANSYS Fluent. The simulation provided pressure and temperature distributions within the jet plume as it expanded and mixed with the surrounding atmosphere. Although contrail contours were not obtained in the present simulations, the pressure and temperature fields could be used to determine contrail favorable regions in the wake based on the Schmidt-Appleman Criterion [3].

Several improvements can be made in future work to enhance the accuracy of contrail modeling.

First, custom field functions or user-defined expressions can be implemented in ANSYS Fluent to evaluate the mixing and saturation point of water vapor in the plume throughout the computational domain. This would allow the solver to identify regions where the critical temperature condition is satisfied and contrail formation is likely.

Second, the current simulations treat the exhaust plume as a single-phase flow without explicitly modeling water vapor. Future studies could include water vapor as an additional species within a multi-component flow model. This would allow simulation of humidity transport and enable more accurate evaluation of saturation conditions within the plume.

Finally, incorporating phase change models and microphysical ice formation mechanisms would allow the direct simulation of contrail formation and evolution rather than relying solely on thermodynamic criteria.

Such improvements would enhance the ability of CFD simulations to predict contrail formation and provide deeper insight into the atmospheric impacts of aircraft emissions and how engine parameters can be changed to mitigate these impacts. Eventually, the focus and purpose of this modeling approach is to remove the need for numerical determinacy of contrail favorable regions and instead move towards a complete framework for CFD-based contrail predictions of various engines.

BIBLIOGRAPHY

[1] D.S. Lee, D.W. Fahey, A. Skowron, M.R. Allen, U. Burkhardt, Q. Chen, S.J. Doherty, S. Freeman, P.M. Forster, J. Fuglestvedt, A. Gettelman, R.R. De León, L.L. Lim, M.T. Lund, R.J. Millar, B. Owen, J.E. Penner, G. Pitari, M.J. Prather, R. Sausen, L.J. Wilcox. "The contribution of global aviation to anthropogenic climate forcing for 2000 to 2018", Atmospheric Environment, Volume 244, 2021, 117834, ISSN 1352-2310

[2] Kärcher, B. Formation and radiative forcing of contrail cirrus. *Nat Commun* 9, 1824 (2018).

[3] Appleman, H. "The formation of Exhaust Condensation Trails by Jet Aircraft". 1953, Bull. Amer. Meteor. Soc., 34, 14-20

[4] Pilie, Roland J., and Jiusto, James E. "A laboratory study of contrails". June 20, 1957, J. Met., 15, pp. 149– 54

[5] Schumann, U. "On conditions for contrail formation from aircraft exhausts", Meteorol. Zeitschrift, N.F.5, 4-23, February 1996

[6] Hanson, H.M., Hanson, H.D. "A reexamination of the formation of exhaust condensation trails by jet aircraft", J. Appl. Meteor., 34, 2400-2405, 1995

[7] Jones, S. M., Haller, W. J., and Tong, M. T., *"An N+3 Technology Level Reference Propulsion System,"* NASA Technical Memorandum NASA/TM-2017-219501, NASA Glenn Research Center, Cleveland, OH, May 2017.

[8] Hill, P., and Peterson, C., *Mechanics and Thermodynamics of Propulsion,* 2nd ed., Addison-Wesley Publishing Company, Reading, MA, 1992.

[9] Jack D. Mattingly, Elements of Propulsion: Gas Turbines and Rockets, Second Edition, American Institute of Aeronautics and Astronautics, Reston Virginia, 2006

[10] J. A. Goff and S. Gratch. “Low-pressure properties of water from -160 to 212 °f. Transactions of the American Society of Heating and Ventilating Engineers”, pages 95–122, 194

[11] Peter, J. L., 1993. “New techniques for contrail forecasting.” AWS/TR—93/001, Air Weather Service, Scott AFB, IL, 26 pp.